Catalysis Letters (2020) 150:2763–2773
https://doi.org/10.1007/s10562-020-03178-z

Investigating the Support Effect for Catalytic Elimination of Methyl Mercaptan: Role of Hydroxyl Groups over Cr-based Catalysts

Yutong Zhao[1] · Dedong He[2] · Dingkai Chen[1] · Jichang Lu[1] · Jie Yu[1] · Jiangping Liu[1] · Xiaohua Cao[1] · Caiyun Han[1] · Yongming Luo[1]

Received: 2 February 2020 / Accepted: 10 March 2020 / Published online: 19 March 2020

Abstract

The support effect for HZSM-5 and Al_2O_3-supported chromium (Cr) catalysts on the catalytic decomposition of methyl mercaptan (CH_3SH) is investigated. Characterization results reveal that the distribution, reducibility, oxidation states and coordination environment of chromium species mightily depend on the nature of support. Al_2O_3 support is covered by surface hydroxyl groups, thus conducing to the formation of monochromatic Cr(VI) species with tetrahedral coordination, which remarkably increases the reducibility and dispersion of chromium species. In contrast, plenty of inactive α-Cr_2O_3 particles are formed on the surface of Cr/HZSM-5 catalyst due to the lack of adequate hydroxyl sites. Furthermore, a positive correlation is established between the content of active Cr(VI) species and the number of surface hydroxyl groups over Cr/Al_2O_3 catalysts. Reactivity data suggest that the addition of chromium species can observably enhance the conversion of CH_3SH for both two supports. More importantly, 5% Cr/Al_2O_3 catalyst features the superior catalytic performance at 400 °C (100% conversion). The promoting effect can be attributed to the high-content hydroxyl groups on Al_2O_3, which are proven to stabilize monochromatic Cr(VI) species. This result also provides evidence for the active sites of CH_3SH decomposition reaction.

Graphic Abstract

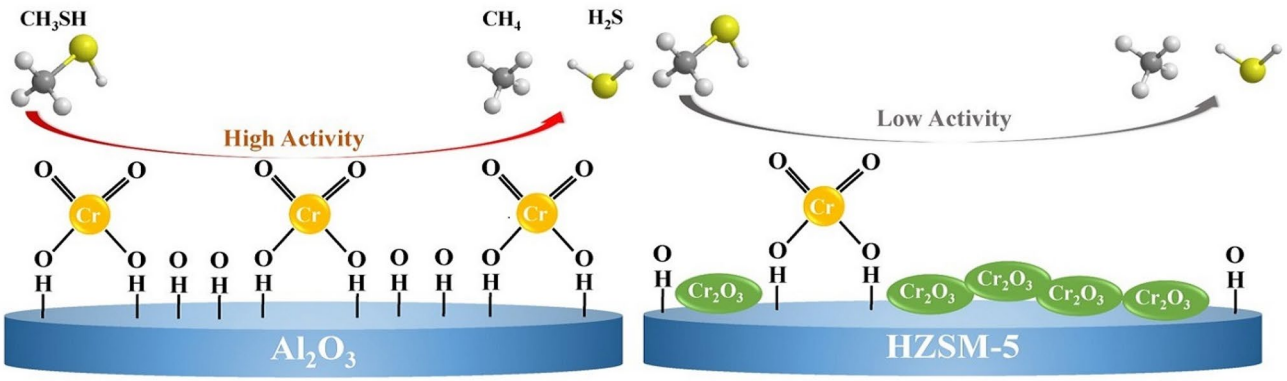

Keywords Sulfur-containing VOC · CH_3SH elimination · Support effect · Active sites · Hydroxyl groups · Cr doping

1 Introduction

Recently, environmental pollution from VOCs (volatile organic compounds) has become an important issue, which has gained sustained attention in the field of environmental protection [1]. As typical sulfur-containing VOCs, methyl mercaptan (CH_3SH) with subtle olfactory threshold and

Electronic supplementary material The online version of this article (https://doi.org/10.1007/s10562-020-03178-z) contains supplementary material, which is available to authorized users.

✉ Dedong He
dedong.he@qq.com

✉ Yongming Luo
environcatalysis@kust.edu.cn

Extended author information available on the last page of the article

high levels of toxicity generally forms in the processes of petroleum refining and environmental pollution control activities [2, 3]. Great trials have been dedicated to exploiting efficient routes for eliminating CH_3SH. Among these methods, catalytic conversion has been extensively investigated in the past years because of many advantages such as high degradation efficiency and less harmful compounds formation [4]. The process of CH_3SH catalytic conversion (M2TH) can be described as the equation: $CH_3SH \rightleftharpoons CH_3SCH_3 + H_2S \rightarrow CH_4 + H_2S$. Dimethylsulfide ($CH_3SCH_3$) is usually formed as the intermediate along with the rupture and formation of H–S and C–S bonds. Consequently, it is necessary to develop suitable and high-performance catalysts for the decomposition of CH_3SH.

Considering that transition metals (such as V, Cr, Mn, Fe, Co, Ni and Cu) oxide catalysts have variable valences, which may have the potential to increase the catalytic activity under the low temperature. Among these transition metal oxide, chromium (Cr) species are commonly used as the active component in several catalytic reaction systems due to its outstanding reducibility and acidity for the removal of VOCs [5, 6]. In these studies, some researchers proposed that Cr(III) species are the active sites for the decomposition of VOCs [7, 8]. But it is also reported that the presence of Cr(VI) is contributed to enhancing catalytic activity for deeply oxidize VOCs [6, 9]. Actually, our previous papers have shown that the reversible modifiability of oxidation states between Ce(VI) and Ce(III) over CeO_2 catalysts was in favor of CH_3SH catalytic decomposition, which is similar to that on Cr-based catalysts with redox cycle [10–12]. Furthermore, our recent studies also have reported that Cr-based catalysts exhibited excellent catalytic behavior in decomposing CH_3SH [13–16]. Although Cr(VI) species have high toxicity, these species could be reduced to low-valence chromium species in the form of Cr_2O_3 or Cr_2S_3 solid phase after converting CH_3SH, thus reducing the harm to the environment. Therefore, primary challenges related to this catalytic system are to stabilize and increase the amount of active Cr(VI) sites which will be able to affect the catalytic activity.

In fact, several studies have been dedicated to inquiry more amount of active chromium species during the synthesis process of catalysts, in particular, through changing the properties of supports. Some former works have also testified that the nature of support has a noteworthy influence in the distribution of chromium species. Kumar et al. studied the oxidation states and coordination environment of active chromium species over Cr-SBA-15 and Cr-Al_2O_3 catalysts, indicating that oligomers with different degrees of nuclearity were generated on γ-Al_2O_3 while SBA-15 contains mainly monomers and α-Cr_2O_3 particles, which caused the diversity of active sites on the different support for dehydrogenation of propane [17]. Su et al. concluded that higher ratios of surface Cr(VI)/Cr(III) could be obtained on the Cr/HZSM-5 catalysts with lower Cr loading, resulting in the enrichment of reducibility for combustion of dichloromethane [18]. Similarly, Ayari et al. pointed out that more amount of amorphous Cr oxide was agglomerated over Cr doped HZSM-5 with different Si/Al ratio, and it further indicated that the formed Cr species depended on the nature of support in selective catalytic reduction (SCR) of NO with ammonia [19]. On the basis of the above findings, it can be assumed that the distribution of chromium species with varied valence states can be tuned by the nature of support, which significantly impacts on the catalytic behavior of obtained catalysts for different reactions.

As commonly applied commercial supports, HZSM-5 and γ-Al_2O_3 are usually adopted as support of preferable selection for the desulfurization processes [20]. However, catalytic activities of these pure supports may be unsatisfactory for the conversion of CH_3SH, thus requiring either heating or enough active sites. Combined with the our previous studies, the redox performance of one active species might be beneficial to reducing the temperature for the complete conversion of CH_3SH. Thus, the introduction of chromium species on HZSM-5 and γ-Al_2O_3 may make up for these defects to increase activity at lower reaction temperatures. To date, nevertheless, almost no study has been focused on the support effect for decomposing sulfur-containing VOCs. Regardless of the fact that various Cr-based catalysts are being developed and evaluated, comprehensive studies between Cr/HZSM-5 and Cr/Al_2O_3 materials also have not been thoroughly studied thus far, especially for eliminating CH_3SH.

Herein, a series of Cr/HZSM-5 and Cr/Al_2O_3 samples by varying chromium contents was employed to understand the role of support in the abatement of CH_3SH and thereby to develop the catalytic behavior of Cr-based catalysts. The physicochemical properties of various samples were analyzed by N_2 adsorption–desorption, XRD, UV–Vis, XPS, H_2-TPR, FT-IR and TG techniques to investigate the distribution of chromium species on HZSM-5 and Al_2O_3. Furthermore, the relationship between the number of surface hydroxyl groups and active Cr(VI) species have been evidently demonstrated.

2 Experimental

2.1 Catalysts Preparation

Zeolite HZSM-5 (Si/Al = 20) was purchased from Fuxu Zeolite Company of China, and γ-Al_2O_3 was obtained from Sinopharm Chemical Reagent Co. Ltd. The commercial HZSM-5 and γ-Al_2O_3 supports were calcined at 550 °C in the air for 5 h to remove impurities. Chromium doped HZSM-5 and γ-Al_2O_3 samples were prepared via an

incipient wetness impregnation method. Firstly, the calculated number of ammonium chromate was dissolved in the deionized water. Then, 5 g of support (HZSM-5 or γ-Al_2O_3) was added into the obtained mixture solution with stirring to ensure that the chromium precursor fully loaded on the support. After impregnation, the catalysts were dried for 12 h at 105 °C followed by calcination in the air for 5 h at 550 °C with a rate of 5 °C/min. The synthesized catalysts were denoted as x% Cr/HZSM-5 and x% Cr/Al_2O_3, where x represents the loading of chromium (x = 1, 5 and 10 wt%).

For dihydroxylation modification, γ-Al_2O_3 supports were calcined in the air at 450, 550, 650, 750 °C for 5 h with a ramp rate of 5 °C/min. Then, 5 wt% Cr (ammonium chromate) was loaded onto the calcined γ-Al_2O_3 with different temperatures by impregnation method similar to the above steps. The final products were denoted herein as Cr/Al_2O_3(y), where y represents the calcined temperature.

2.2 Catalysts Characterization

The specific surface areas and pore volumes of samples could be determined by N_2 adsorption–desorption. ZSM-5 and Cr/HZSM-5 samples were carried out on an ASAP 2020 nitrogen adsorption apparatus. Al_2O_3 and Cr/Al_2O_3 samples were used by NOVA 4200e Surface Area & Pore Size Analyzer. X-ray diffraction (XRD) patterns of obtained catalysts were measured by a Rigaku D/max-1200 diffractometer using Cu Kα radiation (λ = 1.5406 Å) at 40 kV and 30 mA. UV–vis diffuse reflectance spectra (UV–Vis DRS) were recorded with a PERSEE TU-1901 and measured in the region of 250–800 nm at room temperature. X-ray photoelectron spectroscopy (XPS) analyses were carried out on a PHI 5000 Versa Probe II spectrometer. C1 s at 284.6 eV was employed for adjusting binding energy. All infrared spectra were acquired using an IR spectrometer of Bruker Tensor II with KBr pellets in the region of 400–4000 cm^{-1} at room temperature. Thermogravimetric (TG) analysis was recorded on a Mettler-Toledo TGA/DSC (STA449F3) instrument at a heating rate of 10 °C/min from room temperature to 800 °C in nitrogen flow.

H_2-temperature programmed reduction (H_2-TPR) experiments were carried out using a device equipped with a thermal conductivity detector (TCD). Firstly, 0.1 g catalyst was pretreated in a quartz reactor at 100 °C in a flow of H_2/Ar for 1 h. Afterward, H_2-TPR was performed from 100 to 700 °C in H_2/Ar flow with the ramp rate of 10 °C/min.

2.3 Activity Tests

All activity tests for CH_3SH decomposition were measured in a fixed-bed quartz reactor under atmospheric pressure in range 350 °C from 500 °C. An amount of 0.2 g of catalyst with 60–40 mesh size was filled in the reactor. The reactor feed to a CH_3SH/N_2 mixture (1% CH_3SH in N_2) at a rate of 30 mL·min^{-1}. Corresponding reactants were detected via an on-line gas chromatograph (GC) equipped with a flame ionization detector (FID).

CH_3SH Conversion (X_{CH_3SH}) was calculated as follows:

$$X_{CH_3SH} = \frac{C_{[CH_3SH]_{in}} - C_{[CH_3SH]_{out}}}{C_{[CH_3SH]_{in}}} \times 100\%$$

$C_{[CH_3SH]in}$ denotes the CH_3SH concentration in the inlet and $C_{[CH_3SH]out}$ represents the CH_3SH concentration in the outlet.

3 Results

3.1 Catalytic Activity Tests

Figure 1 displays the catalytic activity of HZSM-5, Al_2O_3, 5%Cr/HZSM-5 and 5%Cr/Al_2O_3 catalysts for CH_3SH conversion. The catalytic activity of 0, 1, 5 and 10% Cr loading over different supports is also shown in Fig. S4. Interestingly, it is observed that the performance of obtained catalysts mightily depends on the nature of supports. With respect to the pure supports, the catalytic activity of Al_2O_3 for decomposing CH_3SH is higher than that of HZSM-5. Moreover, the activity improves with the addition of Cr species in comparison to both pure catalysts. In other words, it can be concluded that chromium species are the main active component for converting CH_3SH molecule. Additionally, it is worth noting that there is a great difference in the activity for both Cr-based catalysts with the same loading amounts of about 5 wt% Cr. From Fig. 1, although all Cr-based catalysts reached 100% conversion for CH_3SH, Cr/HZSM-5 catalyst is dramatically less active than Cr/Al_2O_3.

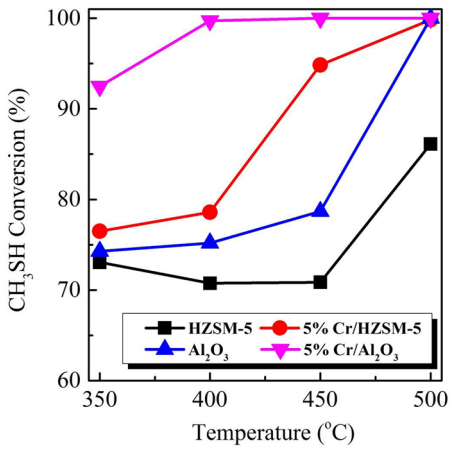

Fig. 1 Catalytic activity of HZSM-5, Al_2O_3, 5%Cr/HZSM-5 and 5%Cr/Al_2O_3 catalysts for CH_3SH conversion

In the case of Cr/Al_2O_3, a decrease of 100 °C is observed already on the conversion temperature of CH_3SH in comparison to the Cr/HZSM-5 sample. The CH_3SH conversion of the four obtained catalysts can be ordered as follows: 5% Cr/Al_2O_3 > 5% Cr/HZSM-5 > Al_2O_3 > HZSM-5, manifesting that the interactions between Cr species and different supports are diverse even with the same loading of Cr. The difference in activity between the Cr/HZSM-5 and Cr/Al_2O_3 catalysts can be interpreted in terms of these textural and structural properties as following characterization results.

3.2 N_2 Adsorption–Desorption

The textural properties of the HZSM-5, Al_2O_3, 5%Cr/HZSM-5 and 5%Cr/Al_2O_3 samples have been measured by N_2 adsorption–desorption isotherms, with the profiles depicted in Fig. 2a, b. According to IUPAC classification, type I isotherms are found for HZSM-5 and 5%Cr/HZSM-5 in Fig. 2a, which is representative of typical microporous materials. Nevertheless, in Fig. 2b, nitrogen adsorption of Al_2O_3 and 5%Cr/Al_2O_3 samples exhibited type IV isotherms, attributed to adsorption on the ordered mesoporous materials. The intercept of the t-plots for HZSM-5 and Cr-doped HZSM-5 samples are 103.17 and 96.78, respectively (Fig. S1). These phenomena reveal that doping Cr does not significantly change the structure of HZSM-5 and Al_2O_3 supports. In addition, the specific surface areas and pore volumes of the catalysts are listed in Table 1. It is observed that loaded chromium catalysts exhibit lower specific surface area, pore diameters and pore volumes than their corresponding supports, suggesting partial CrO_x species may occupy or block the surface and pore of HZSM-5 and Al_2O_3 [21, 22]. Although the specific surface area of Al_2O_3 is smaller than that of HZSM-5, the former exhibits better catalytic behavior. It can be inferred that there are other key factors to influence the performance of the Cr-loaded catalysts besides different texture characteristics.

3.3 Analysis of Phase Compositions

To confirm the phase compositions of Cr species on different supports, XRD measurement was conducted for pure supports, and the corresponding Cr-based catalysts are displayed in Fig. 2c, d. The XRD patterns for the HZSM-5 and

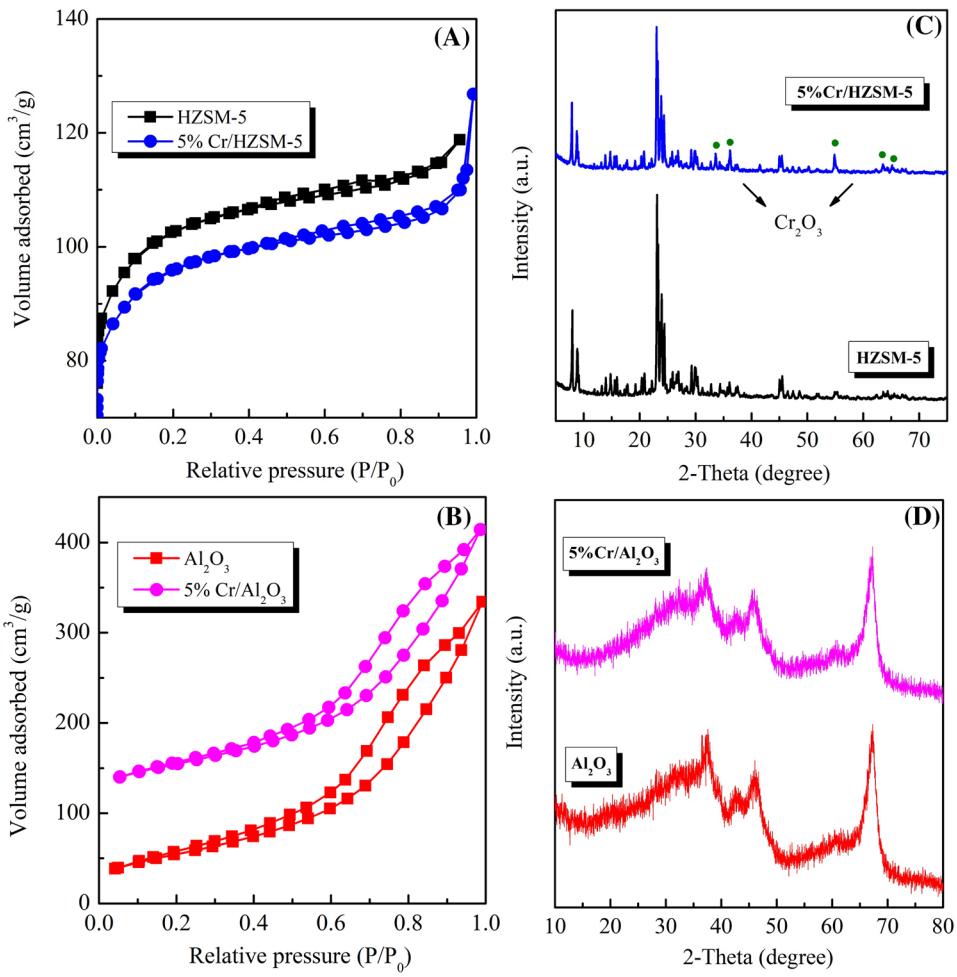

Fig. 2 N_2 adsorption–desorption isotherms of **a** HZSM-5 and 5%Cr/HZSM-5; **b** Al_2O_3 and 5%Cr/Al_2O_3 catalysts and XRD patterns of **c** HZSM-5 and 5%Cr/HZSM-5; **d** Al_2O_3 and 5%Cr/Al_2O_3 catalysts

Table 1 Physicochemical properties of the obtained catalysts

Sample	S_{BET} (m^2g^{-1})	Pore volume (cm^3g^{-1})	H_2 consumption (μmol/g)	Cr(VI) (%)	Cr(III) (%)	Cr(VI)/Cr(III)
HZSM-5	384.3	0.184	–	–	–	–
5% Cr/HZSM-5	361.0	0.177	72	18.78	81.22	0.23
Al_2O_3	281.5	0.521	–	–	–	–
5% Cr/Al_2O_3	243.4	0.491	908.5	39.05	60.95	0.64

Cr/HZSM-5 show well-crystallized MFI zeolitic framework structure as shown in Fig. 2c [23]. Addition of chromium does not change the structure of the zeolite support, while the characteristic peaks of α-Cr_2O_3 (2θ = 33.7°, 36.2°, 54.9°, 63.5° and 65.1°) are presented on Cr/HZSM-5 (JCPDS 38–1479) [24]. Meanwhile, it can be seen from Fig. S2(A) that the intensity of those peaks increases gradually as the Cr loading is increased up to 10 wt%. Additionally, according to Fig. S3, the results of the TEM morphology of HZSM-5 and Cr/HZSM-5 catalysts are in line with the results obtained via XRD. However, in Fig. 2d, three diffraction characteristic peaks of γ-Al_2O_3 and Cr/Al_2O_3 materials reflects at 2θ = 37.7°, 46.0° and 66.9°, corresponding to (211/103), (220/004) and (224) peaks, respectively (JCPDS 00-034-0493) [25]. The introduction of Cr also does not arouse the change of the crystallinity over Al_2O_3 support. Nevertheless, in contrast to Cr/HZSM-5, there is no apparent characteristic peak of CrO_x species for Cr/Al_2O_3 samples. Such behavior can be also observed in 1–10 wt% Cr/Al_2O_3 catalysts from Fig. S2(B), revealing that chromium species are highly dispersed, or the size of CrO_x aggregation is too small to detect in XRD [17, 26]. Amounts of crystalline Cr_2O_3 particles with inactive species agglomerated upon the HZSM-5 support, markedly decreasing the catalytic decomposition activity based on other studies [15]. According to XRD results, it can be considered that the various phase compositions of Cr species could generate on HZSM-5 and Al_2O_3 supports although their loading contents of chromium are similar. Therefore, it is reasonable to deduce that the different composition of chromium species may eventually influence the catalytic performance of obtained catalysts.

3.4 Characterization of the Chromium Species

UV–Vis diffuse reflectance measurements are acquired to identify the coordination environment of Cr species on the different supports, and the results are illustrated in Fig. 3a, b. Obviously, the pure HZSM-5 and Al_2O_3 supports have no absorption bands related to chromium species. Two absorption peaks around 270 and 360 nm appear over both modified catalysts, which can be corresponded with O to Cr(VI) charge transfer transitions of monochromatic in tetrahedral coordination [27]. Moreover, it is seen from Fig. 3a that two intense peaks around 460 and 610 nm in the spectrum of Cr/HZSM-5 derive from the octahedral symmetry transition of CrO_x or Cr_2O_3 clusters [28]. It is particularly mentioned here that the Cr/Al_2O_3 sample has only two bands corresponding to Cr(VI) species in Fig. 3b. This phenomenon has strongly demonstrated that, as for similar Cr loadings, chromium species with various forms disperse on the HZSM-5 and Al_2O_3 supports, which agrees well with the present XRD results.

To understand the effect of supports on CH_3SH abatement, the surface compositions of the Cr-based catalysts can be measured by XPS analysis, and the Cr 2p spectra collected for different supports are depicted in Fig. 3c, d, and the corresponding contents of surface chromium are quantified in Table 1. The results manifest the co-existence of trivalent and hexavalent chromium ions in the case of all analyzed composites. As for both Cr-based catalysts, the binding energy peaks of Cr(III) and Cr(VI) locate at about 576 eV and 578 eV, respectively [29]. Although ammonium chromate is employed as the precursor, parts of Cr(VI) species can be reduced into low oxidation states by ammonia during the calcination process. As shown in Table 1, more than 80% of the total chromium surface ions exist in the oxidation state Cr(III) for Cr/HZSM-5 catalyst. However, in the case of Cr/Al_2O_3, the binding energy peak strength of Cr(VI) species is significantly higher according to Fig. 3d. More importantly, it has been previously reported that Cr(VI) species can be regarded as the active components in favor of catalytic reaction of CH_3SH [13, 14]. Therefore, we can obtain the conclusion that Al_2O_3 support can stabilize a larger amount of Cr(VI) species compared with HZSM-5, but existing a handful of Cr(III) species from Cr_2O_3. This is also in agreement with the results of XRD and UV–Vis. In brief, there is a significant difference in the distribution of Cr(III) and Cr(VI) species in the case of a similar impregnated amount of chromium over HZSM-5 and Al_2O_3 supports, which causes a distinction in the catalytic performance.

3.5 Reducibility of the Cr-based Catalysts

Since the reducibility of Cr-based catalysts plays a key role in catalytic conversion of VOCs, H_2-TPR experiments were performed for both pure supports and their corresponding

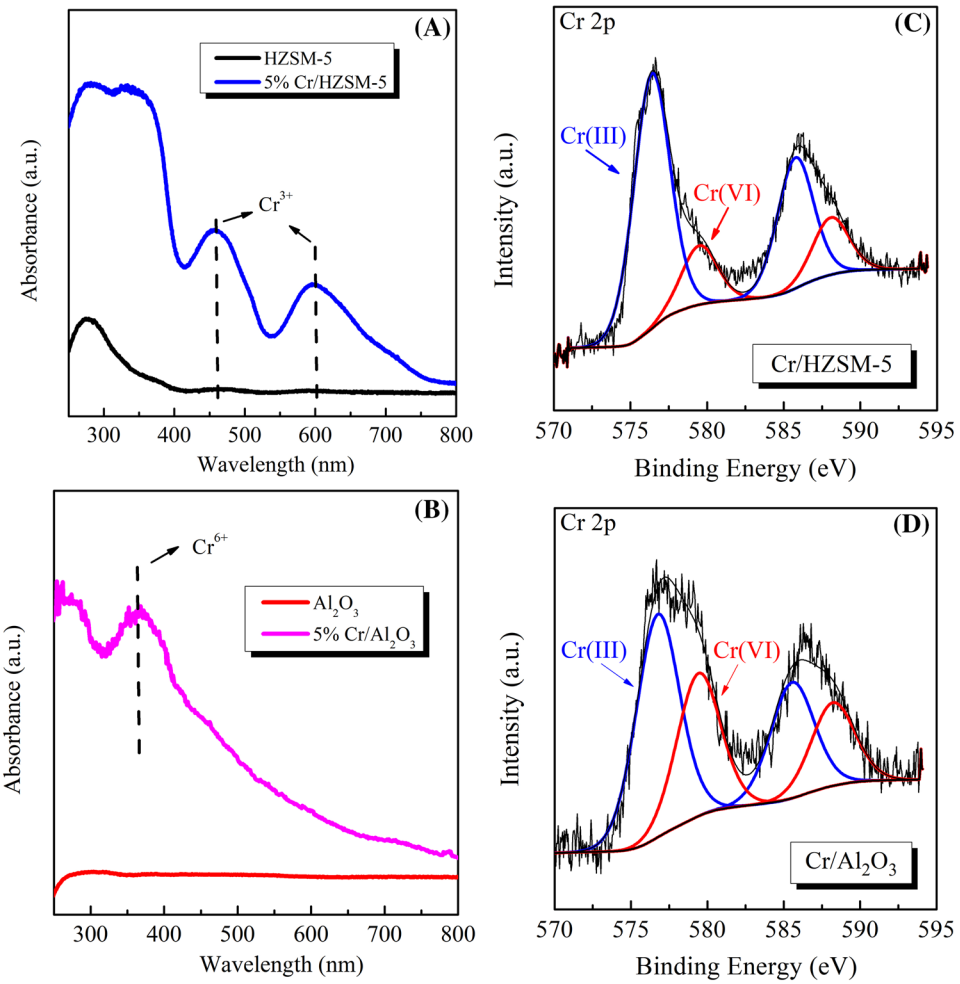

Fig. 3 UV–Vis diffuse reflectance spectra of **a** HZSM-5 and 5%Cr/HZSM-5; **b** Al_2O_3 and 5%Cr/Al_2O_3 catalysts and XPS spectra of Cr 2p on **c** 5%Cr/HZSM-5 and **d** 5%Cr/Al_2O_3 catalysts

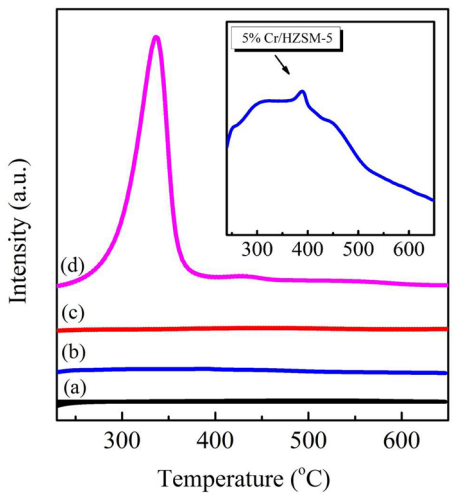

Fig. 4 H_2-TPR profiles of (a) HZSM-5, (b) 5%Cr/HZSM-5, (c) Al_2O_3 and (d) 5%Cr/Al_2O_3

Cr-based samples. As clearly shown in Fig. 4, there are almost no reduction peaks for pure HZSM-5 and Al_2O_3 in the temperature range of 200–650 °C, revealing the inert characteristics of supports [30, 31]. A very small reduction peak of Cr(VI) is found by magnifying the spectral line of the Cr/HZSM-5 (inset), suggesting that only a little Cr(VI) disperses on the surface of HZSM-5 support. In contrast, it is worth noting that for Cr/Al_2O_3 catalyst an intense hydrogen uptake peak due to the reduction of Cr(VI) into Cr(III) appears around 300–400 °C. To obtain more proof, H_2 consumption amounts of primary reduction peak are quantified and displayed in Table 1. Obviously, the H_2 consumption amount of Cr/Al_2O_3 is up to 908.5 μmol/g, which is far more than that of Cr/HZSM-5 catalyst. It is pointed out here that the Cr/Al_2O_3 catalyst has the largest amount of Cr(VI) species, which could result in an improvement of reducibility. Additionally, the Cr(III) species existing in Cr_2O_3 could hardly be reduced into lower oxidize state species, so that the reduction peak of Cr (III) is not observed in the H_2-TPR spectrum from Fig. S4(B). In other words, the hydrogen consumption peak is closely related to the content of Cr (VI) species.

In summary, H_2-TPR analysis is quite consistent with UV–Vis and XPS measurements, testifying strongly that plenty of Cr(VI) disperses on the Al_2O_3 support in comparison with HZSM-5 catalyst. Most importantly, Cr(VI) species are more conducive to CH_3SH decomposition due to its outstanding reducibility, which is considered to be responsible for the highest catalytic performance on Cr/Al_2O_3 catalyst.

3.6 FT-IR Measurement and the Oxygen Properties of the Catalysts

To investigate the surface groups of the obtained catalysts, the FT-IR spectra in a frequency range of 4000–400 cm^{-1} are displayed in Fig. 5. As for the fresh HZSM-5 sample in Fig. 5a, the main vibration frequency peaks at about 450, 560, 800, 1110 and 1230 cm^{-1} can be identified, corresponding to the characteristic of MFI type zeolites [32]. In the case of Al_2O_3 support, the broad bands of Al–O stretching within the scope of 1000–500 cm^{-1} indicate the γ-Al_2O_3 phase. The bands around 734 and 581 cm^{-1} are assigned to the AlO_4 and AlO_6 stretching vibrations of Al–O bond in alumina, respectively. Moreover, the peak at 1450 cm^{-1} can be ascribed to the stretching vibration of Al–OH bands [33, 34]. In addition, an absorption peak at 1650 cm^{-1} observed in both HZSM-5 and Al_2O_3 spectra originates from the bending vibration of OH groups within water molecules, which results from the physically adsorbed water. It should be noted that a broad peak at around 3800–3100 cm^{-1} with a maximum at 3450 cm^{-1} indicates the stretching vibrations of free and bridging surface hydroxyl groups (from inset) [35, 36]. Apparently, the intensity of hydroxyl groups on Al_2O_3 is higher than that on HZSM-5, demonstrating that there are amounts of hydroxyl groups on Al_2O_3 support.

To understand the influence of chromium species in the surface groups on HZSM-5 and Al_2O_3 supports, the FT-IR spectra with a frequency range from 700 to 500 cm^{-1} are displayed in Fig. 7b. As for Cr/HZSM-5 catalyst, the peaks appeared around 550 and 630 cm^{-1} can be designated to the Cr–O distortion vibrations and the characteristic of α-Cr_2O_3 phase, respectively [37, 38]. It also confirms that

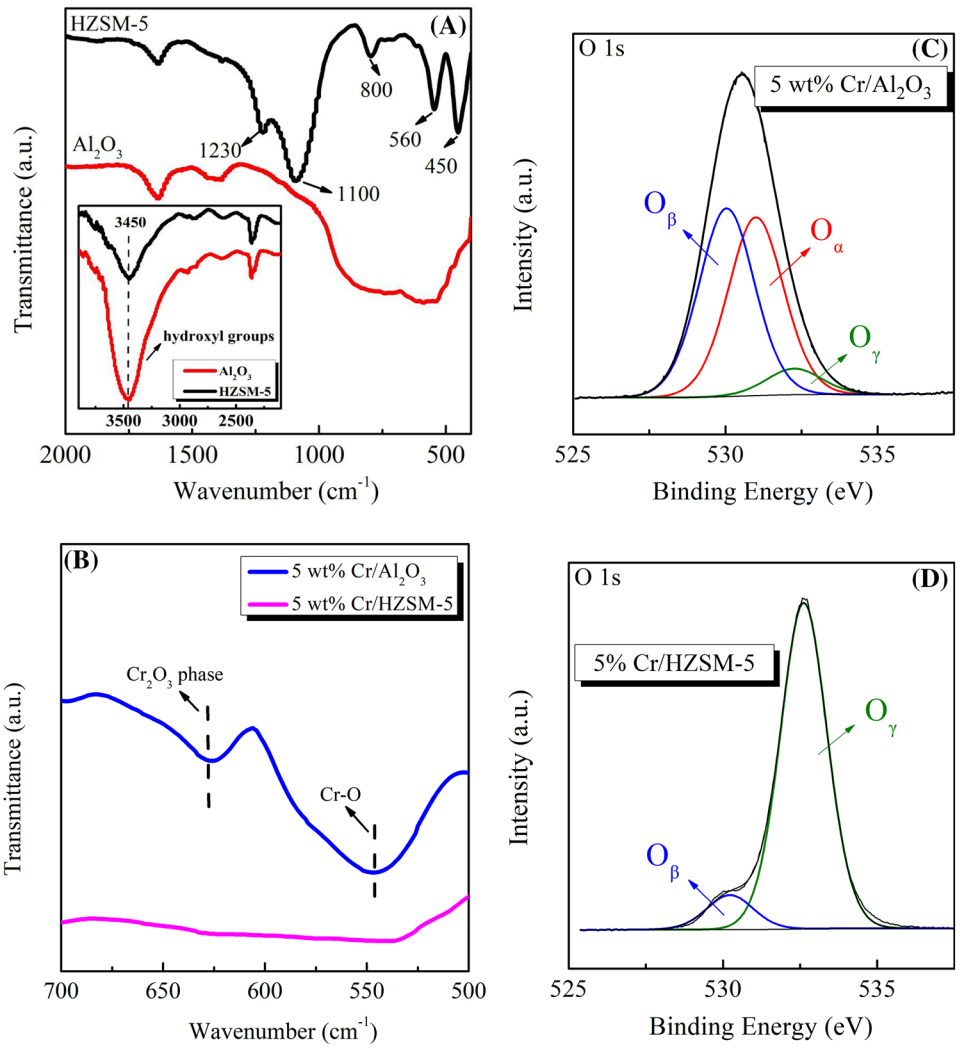

Fig. 5 FT-IR spectra of **a** HZSM-5 and Al_2O_3; **b** 5%Cr/Al_2O_3 and 5%Cr/HZSM-5 and XPS spectra of O 1 s on **c** 5%Cr/Al_2O_3 and **d** 5%Cr/HZSM-5 catalysts

structures of ZSM-5 and Al_2O_3 remain intact after impregnating Cr into support (results not shown). FT-IR analysis is quite consistent with XRD analysis in which α-Cr_2O_3 phases are observed in Cr/HZSM-5 sample.

As displayed in Fig. 5c, d, multiple O 1 s peaks appear for Cr-based samples. For the Cr/Al_2O_3 catalyst, an O 1 s peak at 530.05 eV attributes to the surface lattice oxygen (O_β), and the peak around 531.0 eV can correspond to the surface hydroxyl groups (O_α). Besides, a smaller peak at 532.35 eV assigns to the adsorbed oxygen species (O_γ) [39]. However, for the Cr/HZSM-5 catalyst, both surface lattice oxygen and adsorbed oxygen species are detected. This fact further provides the evidence that Al_2O_3 support contains plenty of surface hydroxyl groups, in accordance with the FT-IR results. As stated in the literatures, the surface hydroxyl groups on the support could react with the chromium species during the synthesis process. The alumina support not only contains plenty of hydroxyl groups but also promotes the formation of more Cr(VI) dispersed on the surface as evidenced by UV–Vis, XPS and H_2-TPR. Consequently, it is believed that there is a close correlation between the intensity of hydroxyl groups and chromium species.

3.7 Relationship Between OH Groups and Cr(VI)

In order to further demonstrate the relationship between the concentration of surface hydroxyl groups and Cr(VI) species of Cr/Al_2O_3 catalysts, relevant experiments and characterizations were designed as follows. The different hydroxyl concentrations can be obtained through varying calcination temperatures of Al_2O_3 support from 450 °C to 750 °C [40], and then all samples are loaded with 5 wt% Cr by impregnation method. Some former works have also reported that TG characterization could be considered to quantitatively analyze the content of hydroxyl groups [41, 42]. As seen in Fig. 6a, the number of hydroxyl groups of each Cr/Al_2O_3 sample under various calcination temperatures are calculated accordingly. It is found that OH amounts have a negative correlation ($R^2 = 0.95$) with increasing calcination temperature of aluminum support. Moreover, the qualitative analysis and calculation of different kinds of surface chromium species

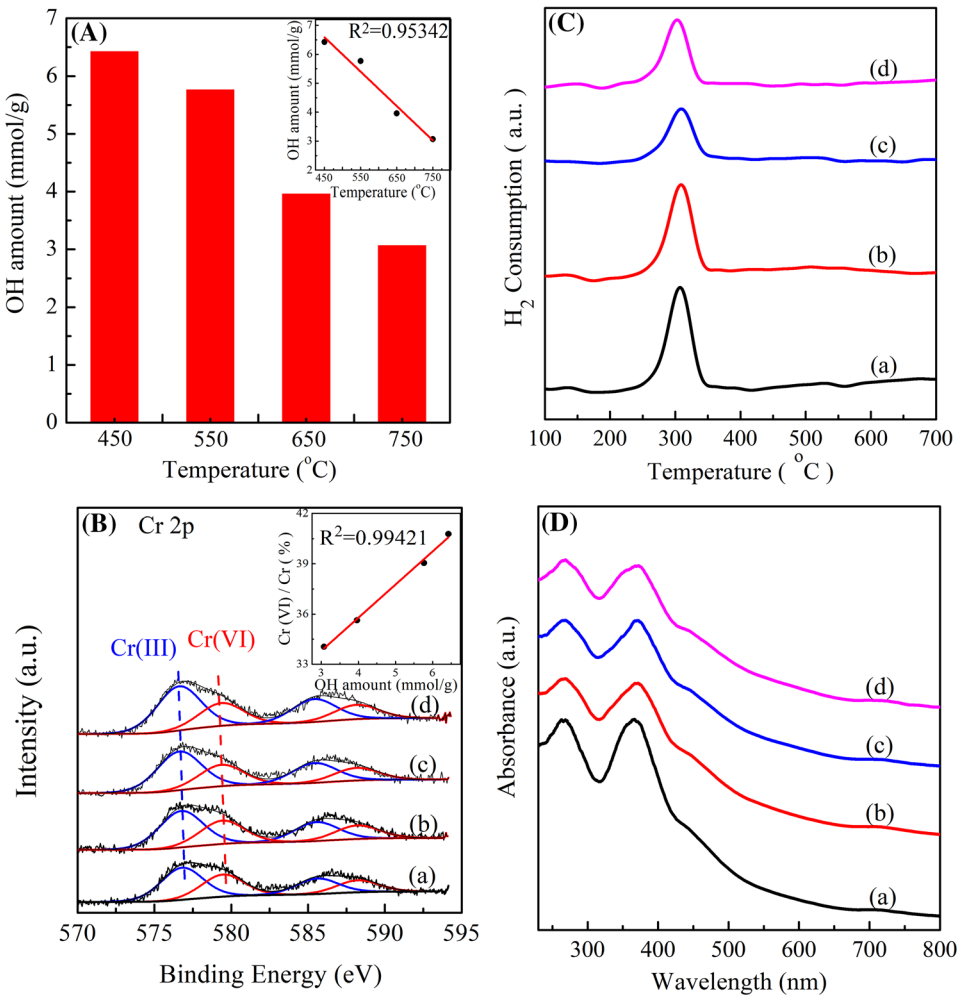

Fig. 6 **a** Surface hydroxyl groups amount quantified by TG versus Al_2O_3 calcination temperature; **b** XPS spectra of Cr 2p and **c** H_2-TPR profiles and **d** UV–Vis spectra of *a* Cr/Al_2O_3(450); *b* Cr/Al_2O_3(550); *c* Cr/Al_2O_3(650); *d* Cr/Al_2O_3(750)

are also carried out by the XPS technique. As presented in Fig. 6b, the Cr 2p spectra evidently prove the coexistence of both Cr(VI) and Cr(III) species. In order to investigate the effect of OH amount on active Cr(VI) species, the surface Cr(VI)/Cr atomic ratios (represent Cr(VI) as a percentage of total chromium) are quantified and displayed in the Inset of Fig. 6b. Notably, the coefficient of determination (R^2) for correlation lines to 0.99, indicating extremely high linearity between the number of surface hydroxyl groups and Cr(VI) species. That is to say, the hydroxyl groups covered Cr/Al_2O_3 samples are beneficial to the stabilization of Cr(VI) species, thus enhancing the catalytic activity. In addition, as shown in Table 2, the binding energy of Cr(VI) species in the Cr $2p_{2/3}$ spectra of Cr/Al_2O_3 samples displays the BE shift from 579.45 eV to 579.35 eV with increasing alumina calcination temperature. This fact shows that the interaction between metal and support is impacted due to the decrease in OH concentration.

To obtain more proof, H_2-TPR and UV–Vis characterizations were carried out. For all of the catalysts, as given in Fig. 6c, the major hydrogen reduction peak is observed around at the temperature range of 200–400 °C. Meanwhile, the intensity of H_2 reduction peak related to Cr(VI) species at low treatment temperature (450 °C) is higher than that at high temperature (550–750 °C), demonstrating that the presence of hydroxyl groups in the support is beneficial to the formation of active Cr(VI) sites with excellent reducibility. Moreover, as proved by UV–Vis spectra in Fig. 6d, both absorption bands corresponding to the tetrahedral coordination of Cr(VI) are more intense and narrower with increasing the calcination temperatures of supports, which is quite consistent with the results of XPS and H_2-TPR. The above statement is directly supported by the fact that the number of surface hydroxyl groups should contribute in a major way to the CH_3SH abatement through anchoring plenty of Cr(VI) species.

4 Discussion

The results in the present work demonstrate that the support effect is a crucial factor for superior Cr-based materials on catalytic decomposition of CH_3SH. Various characterization techniques for Cr/HZSM-5 and Cr/Al_2O_3 prove that the distribution, reducibility, oxidation states and coordination environment of chromium species strongly depend on the property of their supports. The phase compositions and textural properties of Cr-based samples were identified by XRD and N_2 adsorption–desorption, and the surface composition of the Cr species was measured by UV–Vis and XPS. In the case of similar Cr content (5 wt%), Al_2O_3 support mainly contains monochromatic Cr(VI) species in tetrahedral coordination, while crystalline Cr_2O_3 is exclusively generated on the surface of HZSM-5. Moreover, according to H_2-TPR studies, hydrogen consumption is related to the Cr(VI) species, which provides plenty of active sites. Meanwhile, FT-IR analysis shows that the concentration of surface hydroxyl groups in alumina is more than that in HZSM-5 support. Most importantly, these abundant hydroxyl groups on the support play a considerable role in the distribution of chromium. As evidenced by TG and XPS characterization results, it demonstrates that Cr(VI) species can be anchored through reacting with hydroxyl groups, which prevents the generation of inactive α-Cr_2O_3 phase over Al_2O_3 support. In other words, those Cr(III) species as Cr_2O_3 particles are sufficiently stable and difficult to interact with OH groups. Hence, as shown in Fig. 7, Cr(III) as the dominant species exist on the HZSM-5 support because of the lack of sufficient hydroxyl sites. The main products of decomposing CH_3SH are hydrogen sulfide (H_2S) and methane (CH_4) [13].

The 5% Cr/Al_2O_3 catalyst produces the highest CH_3SH conversion rate because (1) it has a good deal of active monochromatic Cr(VI) species with excellent reducibility, decreasing the formation of Cr_2O_3 crystalline; and (2) Al_2O_3 support has enough surface hydroxyl groups, which can be able to anchor active Cr(VI) species.

5 Conclusions

In summary, a series of Cr-based catalysts supported HZSM-5 and Al_2O_3 were prepared by the incipient wetness impregnation method and characterized by N_2 adsorption–desorption, XRD, XPS, UV–Vis, H_2-TPR, FT-IR and TG techniques to investigate the effect of the supports on

Table 2 Surface composition of Cr/Al_2O_3 catalysts with different calcination temperature

Sample	Cr(VI)		Cr(III)		Cr(VI)/Cr(III)
	Content (%)	Binding energy (eV)	Content (%)	Binding energy (eV)	
Cr/Al_2O_3(450)	40.79	579.45	59.21	576.8	0.69
Cr/Al_2O_3(550)	39.05	579.42	60.95	576.75	0.64
Cr/Al_2O_3(650)	35.63	579.36	64.37	576.63	0.55
Cr/Al_2O_3(750)	34.05	579.35	65.95	576.6	0.52

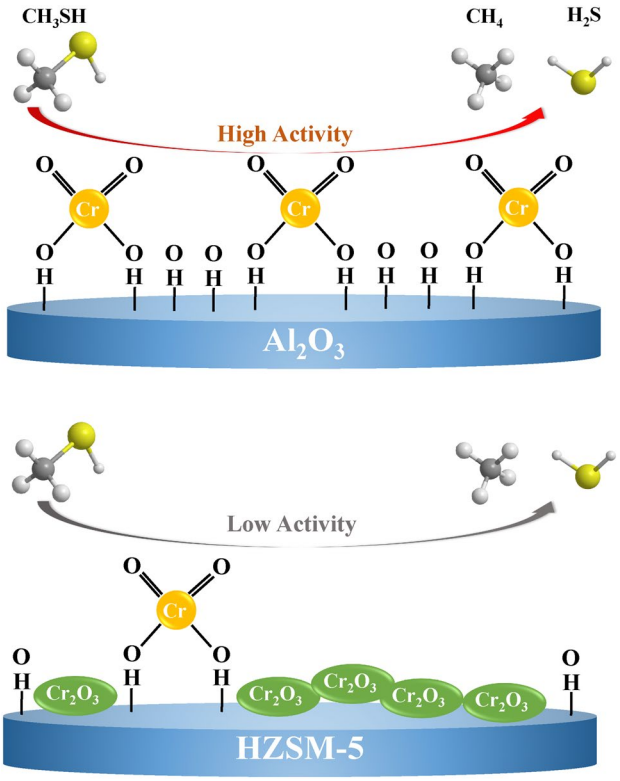

Fig. 7 Diagram for the structure and distribution of Cr species over HZSM-5 and Al_2O_3

eliminating CH_3SH. On the basis of the results and discussion, the following conclusions can be drawn:

(1) It reveals that the dispersion of chromium species depends on the nature of the support, leading to differences in the catalytic conversion of CH_3SH.

(2) In terms of 5 wt% Cr/Al_2O_3, monochromatic Cr(VI) species with tetrahedral coordination are the main component of the Al_2O_3 support. In contrast, crystalline Cr_2O_3 is easier to produce on the 5 wt% Cr/HZSM-5.

(3) Plenty of surface hydroxyl groups covering on the Al_2O_3 support can anchor Cr(VI) species with excellent reducibility, resulting in higher activity of the catalysts. The concentration of OH groups is found to be linearly relative to active Cr(VI) species.

(4) It is deduced that the best performance of Cr-based catalyst can be tailored by providing a sufficient amount of surface hydroxyl groups to anchor the maximum amount of Cr(VI) cations.

Acknowledgements The National Natural Science Foundation of China (21667016, U1402233, 21767016 and 21267011) is gratefully acknowledged for financial support to this research work.

Compliance with Ethical Standards

Conflicts of interest The authors declare no conflicts of interest.

References

1. He C, Cheng J, Zhang X et al (2019) Chem Rev 119:4471–4568
2. He D, Zhao Y, Yang S et al (2018) Chem Eng J 336:579–586
3. Lu J, Hao H, Zhang L et al (2018) Appl Catal B Environ 237:185–197
4. Chen D, Zhang D, He D et al (2018) Chin J Catal 39:1929–1941
5. Abdullah A, Bakar M, Bhatia S (2006) J Hazard Mater 129:39–49
6. Yang P, Xue X, Meng Z et al (2013) Chem Eng J 234:203–210
7. Sinha AK, Suzuki K (2005) Angew Chem Int Ed 44:271–273
8. Cavania F, Koutyreva M, Trifiròa F et al (1996) J Catal 158:236–250
9. Yang P, Xue X, Meng Z et al (2015) Appl Catal B Environ 162:227–235
10. Chen D, He D, Lu J et al (2017) Appl Catal B Environ 218:249–259
11. He D, Wan G, Hao H et al (2016) Chem Eng J 289:161–169
12. He D, Hao H, Chen D et al (2017) Catal Today 281:559–565
13. He D, Zhang L, Zhao Y et al (2018) Environ Sci Technol 52:3669–3675
14. Zhao Y, Lu J, Chen D et al (2019) New J Chem 43:12814–12822
15. He D, Yu J, Mei Y et al (2018) Catal Commun 112:31–34
16. Yu J, He D, Zhao Y et al (2020) Mater Chem Phys 239:121952
17. Kumar MS, Hammer N, Ronning M et al (2009) J Catal 261:116–128
18. Su J, Yao W, Liu Y et al (2017) Appl Surf Sci 396:1026–1033
19. Ayaria F, Mhamdi M, Álvarez-Rodríguez J et al (2013) Appl Catal B Environ 134–135:367–380
20. Subhan F, Aslam S, Yan Z et al (2018) Chem Eng J 354:706–715
21. Cheng Y, Zhang F, Zhang Y et al (2015) Chin J Catal 36:1242–1248
22. Michorczyk P, Pietrzyk P, Ogonowski J (2012) Micropor Mesopor Mat 161:56–66
23. Cheng Y, Miao C, Hua W et al (2017) Appl Catal A Gen 532:111–119
24. Ye N, Li Y, Yang Z et al (2019) Appl Catal A Gen 579:44–51
25. Liu Q, Gu F, Lu X et al (2014) Appl Catal A Gen 488:37–47
26. Scierka S, Houalla M, Proctor A et al (1995) J Phys Chem C 99:1537–1542
27. Baek J, Yun H, Yun D et al (2012) ACS Catal 2:1893–1903
28. Asghari E, Haghighi M, Rahmani F (2016) J Mol Catal A Chem 418–419:115–124
29. Sun M, Du X, Wang H et al (2011) Catal Lett 141:1703–1708
30. Du W, Yin L, Zhuo Y et al (2015) Fuel Process Technol 131:403–408
31. Llunga AK, Meijboom R (2017) Appl Catal B Environ 203:505–514
32. Rahmani F, Haghighi M, Mohammadkhani B (2017) Micropor Mesopor Mat 242:34–49
33. Priya SS, Kumar VP, Kantam ML et al (2014) Catal Lett 144:2129–2143
34. Tabesh S, Davar F, Loghman-Estarki MR (2018) J Alloy Compd 730:441–449
35. Lan S, Guo N, Liu L et al (2013) Appl Surf Sci 283:1032–1040
36. Li GC, Liu YQ, Liu CG (2013) Micropor Mesopor Mat 167:137–145
37. Mahmoud HR (2014) J Mol Catal A Chem 392:216–222
38. He D, Zhang Y, Yang S et al (2019) ACS Sustain Chem Eng 7:3251–3257

39. Boningari T, Ettireddy PR, Somogyvari A et al (2015) J Catal 325:145–155
40. Li Y, Xu J, Qian M et al (2019) Environ Sci Pollut Res 26:15373–15380
41. Ek S, Root A, Peussa M et al (2001) Thermochim Acta 379:201–212
42. Mueller R, Kammler HK, Wegner K et al (2003) Langmuir 19:160–165

Affiliations

Yutong Zhao[1] · Dedong He[2] · Dingkai Chen[1] · Jichang Lu[1] · Jie Yu[1] · Jiangping Liu[1] · Xiaohua Cao[1] · Caiyun Han[1] · Yongming Luo[1]

[1] Faculty of Environmental Science and Engineering, Kunming University of Science and Technology, Kunming 650500, People's Republic of China

[2] Faculty of Chemical Engineering, Kunming University of Science and Technology, Kunming 650500, People's Republic of China